

Electrosprayed catalyst layers based on graphene–carbon black hybrids for the next-generation fuel cell electrodes

Lale Işık Şanlı¹, Begüm Yazar², Vildan Bayram², and Selmiye Alkan Gürsel^{1,2,*}

¹Sabancı University Nanotechnology Research and Application Center (SUNUM), Sabancı University, Istanbul 34956, Turkey

²Faculty of Natural Science and Engineering, Sabancı University, Istanbul 34956, Turkey

Received: 2 July 2016

Accepted: 12 October 2016

Published online:

25 October 2016

ABSTRACT

Here, we report a novel electrode structure with graphene and graphene–carbon black hybrids by electrospraying for polymer electrolyte membrane fuel cells. After syntheses of platinum (Pt)/partially reduced graphene oxide (rGO) and Pt/rGO/carbon black (CB) hybrid electrocatalysts, suspensions of synthesized electrocatalyst inks were prepared with Nafion[®] ionomer and poly(vinylidene fluoride-*co*-hexafluoropropylene) and electrosprayed over carbon paper to form electrodes. Electrosprayed catalyst layer exhibited uniform and small size Pt distribution. As the graphene content increases micrometer-sized droplet, pore formation and surface roughness of the electrode increase. Thus, an open porous electrode structure which is favorable for mass transport is achieved by electrospraying. The maximum power densities, 324 mW cm⁻² for Pt/rGO and 441 mW cm⁻² for Pt/rGO/CB electrosprayed electrodes, were achieved at a relatively low catalyst loading.

Introduction

Polymer electrolyte membrane (PEM) fuel cells draw much attention due to its pollution-free operation in transportation. However, the major limiting factor in PEM fuel cell commercialization is the use of precious and costly platinum (Pt) metal as the electrocatalyst [1]. There are efforts for the development of Pt-free electrocatalysts; however, there is no remarkable power density that meets automotive targets [2]. Since the main goal is to lower Pt loading without losing the fuel cell

performance [3], several techniques have been evolved such as vacuum deposition, sputtering, supercritical deposition, colloidal deposition, reactive spray deposition and electrodeposition methods to have efficient use of Pt [4–9]. In addition to these, electrospraying is a promising technique that leads to electrostatic deposition of the catalyst ink with uniform distribution and efficient utilization of electrocatalyst [10–12]. Moreover, electrospraying method was employed previously to fabricate porous graphene electrodes for supercapacitor applications [13].

Address correspondence to E-mail: selmiye@sabanciuniv.edu

Besides electro spraying technique, graphene is employed as the Pt support to form a novel electrode structure in this study. Although commercial carbon blacks have been regarded as the most extensively used support for Pt, other supports including carbon nanotubes [14–16] and their composites with conducting polymers [17], carbon xerogel and carbon aerogel [18], carbon nanofibers [19], and graphene [20–22] have been utilized previously. Unsupported Pt nanoparticles were also employed as the catalysts for fuel cells as well [8, 22].

Graphene and nitrogen-doped graphene have many attracting features including high surface area and excellent conductivity [23, 24]. However, due to the 2-dimensional (2D) nature of graphene, it tends to stack through π - π interaction [23, 25]. The stacking may cause a higher resistance for diffusion of reactant gases, which retards the catalytic reaction at higher potential range and slow oxygen diffusion. Thus, graphene-carbon black hybrid supports can be a promising alternative as Pt support [26, 27].

In this manner, our group desired to take the advantage of graphene-carbon black (CB) hybrid support morphology and electro spraying technique to alter the PEM fuel cell performance. Recently, we have reported graphene-containing fibrous structures formed by electro spinning [28, 29]. In literature, there are several studies about graphene hybrid supports for Pt, yet, to the best of our knowledge, hybrid structure was formed by mechanical mixing of Pt/graphene electrocatalyst with pristine carbon black or commercial Pt/CB and graphene [26, 30]. However, in our study, Pt/partially reduced graphene oxide (rGO)/CB electrocatalysts were synthesized by mechanical homogenizing of carbon components (rGO and CB). The chemical reduction was employed in the presence of a Pt precursor to form supported Pt nanoparticles on the hybrid support [31, 39]. By this approach, CB was used as an intercalating agent to have higher Pt utilization and better transport of reactants and by-product.

Moreover, synthesized Pt/rGO and Pt/rGO/CB hybrid electrocatalysts mixed with Nafion[®] ionomer and the hydrophobic polymer, poly(vinylidene fluoride-*co*-hexafluoropropylene) (PVDF-*c*-HFP) to have homogenous dispersion in this study. We then used electro spraying technique to apply as-prepared dispersion as the catalyst layer onto the carbon paper (which is also named as gas diffusion layer). PVDF-*c*-HFP was introduced into the catalyst layer to increase

the hydrophobicity of the catalyst layer to retain the balance between high electrochemical surface area and water management issues [32–34]. The low amount of hydrophobic polymer in the electro sprayed electrode structure can balance the open pore structure by creating hydrophobic pores to wick the liquid water away from the catalyst layer through the capillary action so that the mass transport losses mostly coming from cathode side can be improved.

Electro spraying provides an efficient route to fabricate the thin-film electrode of graphene-based materials [30, 35–37, 51, 52]. In our study, the electro spray deposition could continuously proceed without clogging the nozzle and the resulting Pt loading could be controlled. These electrodes showed good uniformity, possessing an open and layered morphology without any macro-aggregation, as shown in scanning electron microscopy (SEM) images. The porosity of the electrodes is also examined via mercury porosimeter to find effect of electrode morphology. Besides we present PEM fuel cell performances of Pt/rGO and Pt/rGO/CB hybrid electro sprayed electrodes.

Experimental

Materials

The graphite flakes, poly(vinylidene fluoride-*co*-hexafluoropropylene) (PVDF-*c*-HFP) (MW 455 kDa), *N,N* dimethylformamide (DMF), potassium permanganate (KMnO₄), sulfuric acid (H₂SO₄), phosphoric acid (H₃PO₄), hydrochloric acid (HCl), hydrogen peroxide (H₂O₂), chloroplatinic acid (H₂PtCl₆), and ethylene glycol (HOCH₂CH₂OH) were purchased from Sigma-Aldrich. Vulcan XC-72 was supplied from Fuel Cell Earth LCC. All chemicals were used without further purification.

Synthesis of Pt/rGO and Pt/rGO/CB hybrid electrocatalysts

In this study, GO was synthesized by an improved Hummers method [38, 39]. Carbon components (0.5 mg/mL) and H₂PtCl₆ (0.5 mg/mL) were ultrasonicated with DI water for 30 min. The weight ratio of rGO to CB as the hybrid support was arranged as shown in Table 1. The synthesis of the hybrid electrocatalysts was explained in our previous study [38].

Table 1 Hybrid electrocatalyst coding according to rGO-to-CB weight ratios (w:w %)

Electrocatalyst	rGO:CB (w:w %)
ES00 (Pt/CB)	0:100
ES25 (Pt/rGO/CB)	25:75
ES50 (Pt/rGO/CB)	50:50
ES75 (Pt/rGO/CB)	75:25
ES100 (Pt/rGO)	100:0

Preparation of electrospaying dispersions

Electrospaying dispersions employed as electrode inks were prepared by mixing of PVDF-*c*-HFP, Nafion[®] ionomer solution, and previously synthesized Pt/rGO or Pt/rGO/CB catalyst. The total solid-to-solvent ratio of 15:85 (w:w) and solid content, Pt/rGO/CB: Nafion[®]: PVDF-*c*-HFP, weight ratio of 65:23:12 were fixed [40]. After dissolving PVDF-*c*-HFP in DMF to form a solution by stirring 48 h, Pt/rGO/CB and Nafion[®] solution was sonicated for 1 h and mixed with polymer solution and left 48 h stirring.

Electrode preparation

The prepared electrospaying dispersion was then loaded into a syringe and fed through a Hamilton needle (18 PS) at a feeding rate of syringe pump (New Era Pump Systems-NE-300) 0.1 mL/min. The applied voltage (Gamma-High Voltage Power Supply, ES30P-20 W) was 15 kV, and the distance from the metallic needle to the surface of the collector was 10 cm. The electrospayed droplets were collected onto carbon paper (AvCarb[®] MGL190 in 190 μ m thickness), which was attached to the metallic flat surface. Finally, electrodes were dried for 24 h at room temperature. For the comparison, an air-sprayed electrode was also prepared same as in our previous study [31, 39].

Measurements

Characterization of electrospayed electrodes

The morphologies of electrospayed micrometer-size droplets were characterized by using SEM (Jeol JSM 6010 LV and Supra 35VP Leo, Germany). Pt particle size and distribution were investigated by using

high-resolution-transmission electron microscopy (JEOL 2100 JEM HR-TEM). Contact angle measurements were performed on the 2×2 cm² electrospayed electrodes. The contact angle measurements were done by Attension Theta Lite model optic tensiometer. For each measurement, a 50 μ L deionized water droplet was made by placing the tip of the syringe close to the electrode surface. The water droplet then attached to the sample surface. Before the water droplet attached to the sample surface, the wetting process was recorded until no significant change at the surface was observed any more. The contact angle of five different spots of the electrode was recorded and average was reported. Porous structure of the electrodes was analyzed by using a mercury porosimeter (Micromeritics Autopore 9500). Porous structures of the GDLs were analyzed by using a mercury porosimeter (Micromeritics Autopore 9500). In order to perform analysis, small pieces of a GDL were weighed and loaded onto a penetrometer which consists of a sample cup integrated with a metal-clad and glass capillary stem, followed by outgassing from a GDL in a vacuum. Then the penetrometer was automatically filled with mercury. Pore size distribution (PSD) curve was determined from the mercury intrusion data, i.e., the volume of mercury penetrating the pores versus the applied pressure.

Membrane electrode assembly (MEA) fabrication and fuel cell testing

MEAs with active area of 25 cm² were prepared by hot-pressing of a pre-conditioned membrane (Nafion[®] NR211) between two previously prepared electrodes at 120 $^{\circ}$ C at 533.8 kPa for 3 min. The fabricated MEA was placed inside the single fuel test cell and temperature was adjusted to desired values at 100 % relative humidity. Hydrogen and oxygen were supplied to the cell at stoichiometric ratios 1.5 and 2, respectively. The fuel cell test was conducted via Scribner 850E fuel cell test system and testing cell. The single cell has graphite flow fields with precision machined, serpentine flow-pattern. Both load unit and humidification system were controlled by Scribner testing system software. The fuel cell measurements were carried out at 50–60 and 80 $^{\circ}$ C under 150 kPa back pressures. The current–voltage data were recorded after steady state was achieved in galvanostatic mode.

Results and discussion

Morphology of electrospayed electrodes

Figure 1 shows the morphology of electrodes with varying rGO to Vulcan XC-72 weight ratios (as given in Table 1). The SEM micrographs with the same magnification show the morphology of the catalyst layer onto the carbon paper. The electrode prepared by electrospaying Pt/CB electrocatalyst, ES00, exhibited compact and less porous structure (Fig. 1a). Roughness of the catalyst layer increases as the rGO is introduced to the support (Fig. 1b). Since electrospaying relies on electrostatic forces to repel micrometer-sized droplets from a charged liquid. Micrometer-size droplets are formed in the catalyst layer, as seen in Fig. 1c, d [52]. With the hybrid morphology of rGO and CB, porous and less compact structure which is extremely desirable for a catalyst layer was obtained. Since 3-dimensional CB acts as a spacer and disturbs the compact structure of rGO, electrospaying prevents compactness like in commercial electrode structure (Fig. 1g). However, in the case of electrode formed from Pt/rGO alone, there is no micrometer-sized droplet formation due to the 2D structure of graphene (Fig. 1e). We expect that the structure obtained via electrospaying of rGO and CB hybrid will enhance the reactant gases reaching to the electrocatalyst surface. Moreover, that improved mass transport will contribute to increased electrochemical reaction rates which results in a pronounced PEM fuel cell performance [41–43]. Figure 1f demonstrates the freeze-fractured cross section of the electrode based on Pt/rGO/CB hybrid catalyst. It indicates that the catalyst layer can reach into the deeper region of the carbon paper in order that more electrocatalyst surface available for electrochemical reactions. Moreover, Fig. 1f shows that there are no un-contact regions between catalyst layer and carbon paper.

TEM micrographs (Fig. 2) revealed the Pt formation, its particle size, and distribution. TEM samples were prepared during electrospaying process via droplet formation on a copper grid. In the case of Pt/rGO electrocatalyst, a wide-range uniform distribution of Pt domains that anchored on graphene with small particle size ($1.5 < D < 2.5$ nm) was achieved (Fig. 2b). In the case of Pt/rGO/CB hybrid electrocatalyst, small $0.5 < D < 1.5$ nm particle size with very low variation was obtained (Fig. 2d). The small

Figure 1 SEM micrographs of **a** ES00, **b** ES25, **c** ES50, **d** ES75, **e** ES100, **f** freeze-fractured cross section of ES50, **g** commercial electrode with blading, **h** cracks on the surface of electrode.

particle size and homogenous Pt particle distribution that support the electrode performance are also other advantages of the hybrid structure of the carbon support [43].

Wettability of the electrospayed electrodes

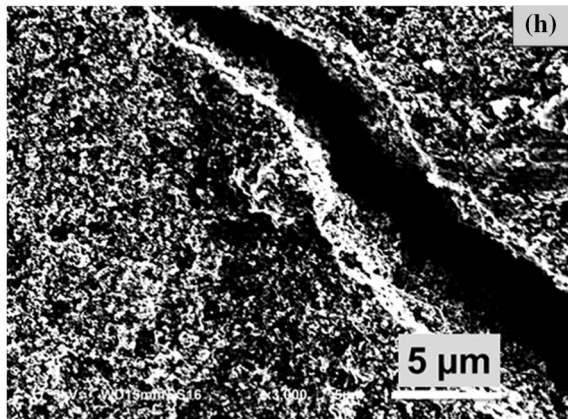
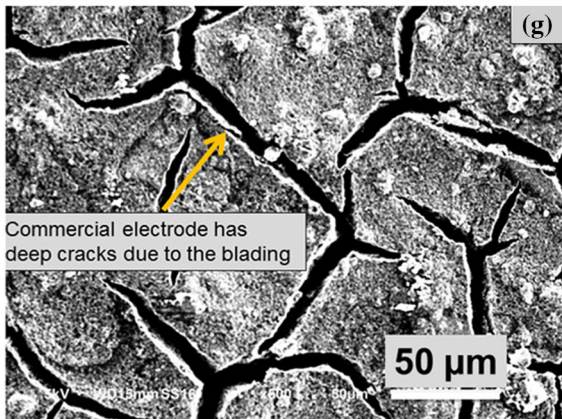
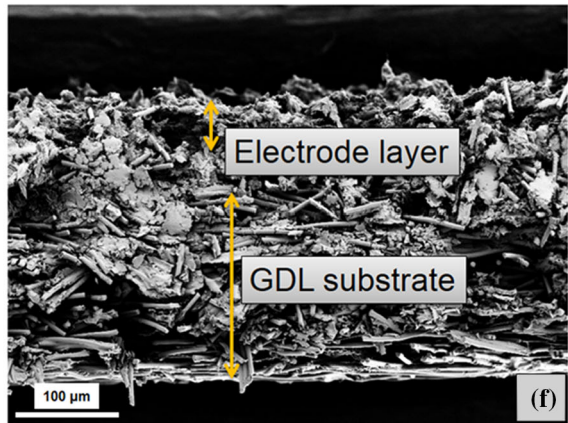
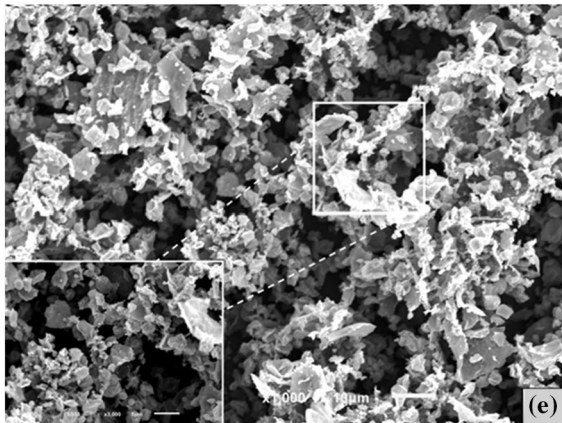
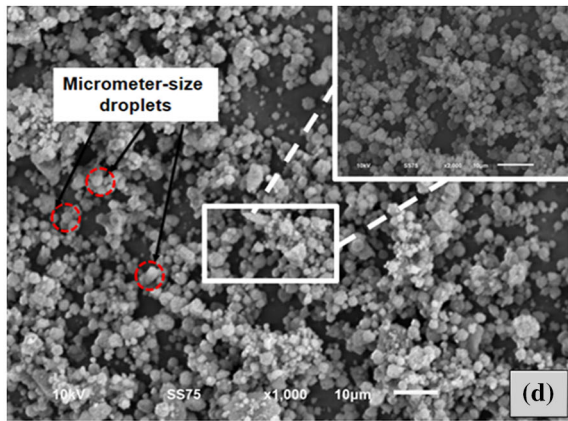
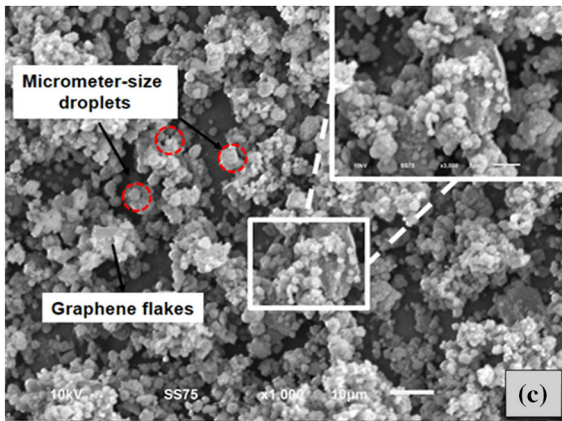
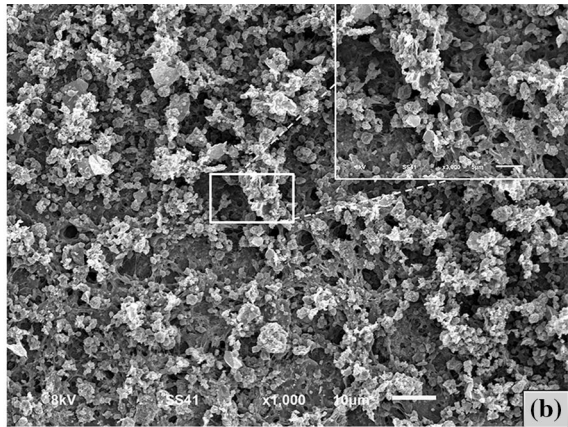
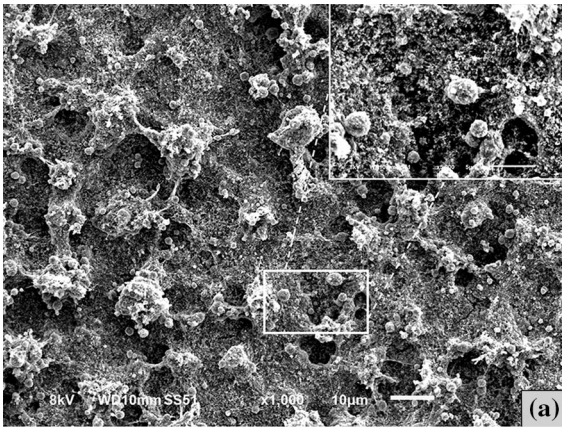
Figure 3 shows the image of the water droplet on each electrode to measure the contact angle and hydrophobicity of the electrospayed electrodes prepared from inks made out of synthesized hybrids electrocatalysts. Electrospayed electrodes of ES00, ES25, ES50, ES75, and ES100 electrocatalysts have varying rGO content in the electrodes as shown in Table 1. Figure 3 shows that contact angle reaches a maxima at 50 wt% rGO content in the hybrid electrocatalyst structure than it slightly decreases; moreover, it is still larger than that of pure Pt/CB (Sample ES00). Thus, the results show that the wettability of the catalyst layer is improved by the addition of hydrophobic rGO to a certain concentration; ES50 and ES75 have the highest contact angle which is the indication of the hydrophobicity of the electrode layer. However, graphene tends to restacking due to the 2-dimensional structure, and contact angle reduces in case of flatter surface. (Fig 1d).

Porosity of the electrospayed electrodes

Because the catalyst layers are porous structures, the influence of the pore size distribution must be taken into account. The pore size between 3 nm and 1100 μm could be measured with operating up to 60,000 psi in our mercury porosimeter [44–46]. Table 2 lists the porosity, average pore diameter, and mean pore diameter for the commercial electrode, pristine carbon paper, and the electrospayed fuel cell electrodes. All pore characteristics were estimated from the analyses of mercury intrusion data, and the average pore diameter ($d_{p,ave}$) was determined using the Carman-Kozeny theory [45].

$$d_{p,ave} = \frac{4V_t}{A_t}$$

where V_t and A_t denote the total instruction volume and total pore surface area in the electrodes,



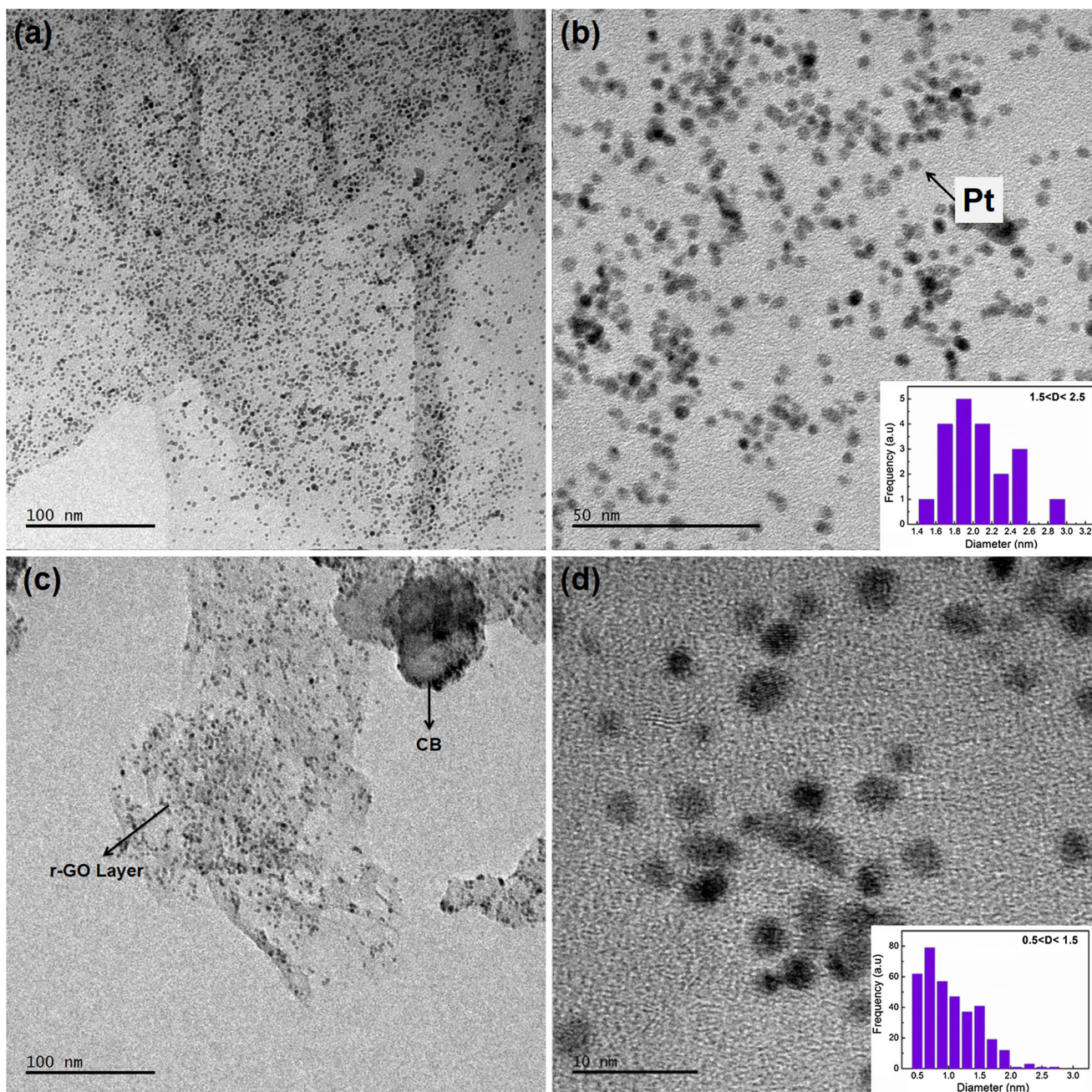


Figure 2 TEM micrographs of **a, b** Pt/r-GO electrocatalyst (ES100) **c, d** Pt/r-GO/Vulcan XC-72 hybrid electrocatalyst (ES50).

respectively. As summarized in Table 2, the mean pore diameter ($d_{p,mean}$), $d_{p,ave}$, and porosity for neat carbon paper are larger among all samples. The porosity of the carbon paper is measured as 77 % in our study that is almost same as the manufacturer specification (78 %) [46]. The porosity of carbon paper reduced to 67 and 71–71 % for commercial electrode and electrospayed electrodes, respectively. Moreover, the average pore diameter of

electrospayed electrodes decreased significantly. Although ES00 (pure CB) and ES100 (100 % rGO) electrospayed electrodes have the same average pore diameter, hybrid electrospayed electrodes exhibited smaller average pore diameter compared to ES00 and ES100. Moreover, average pore diameter of carbon paper decreased remarkably from 23 to 0.5 and 6 μm for commercial electrode and electrospayed electrodes (ES50), respectively. Figure 4 shows the PSD

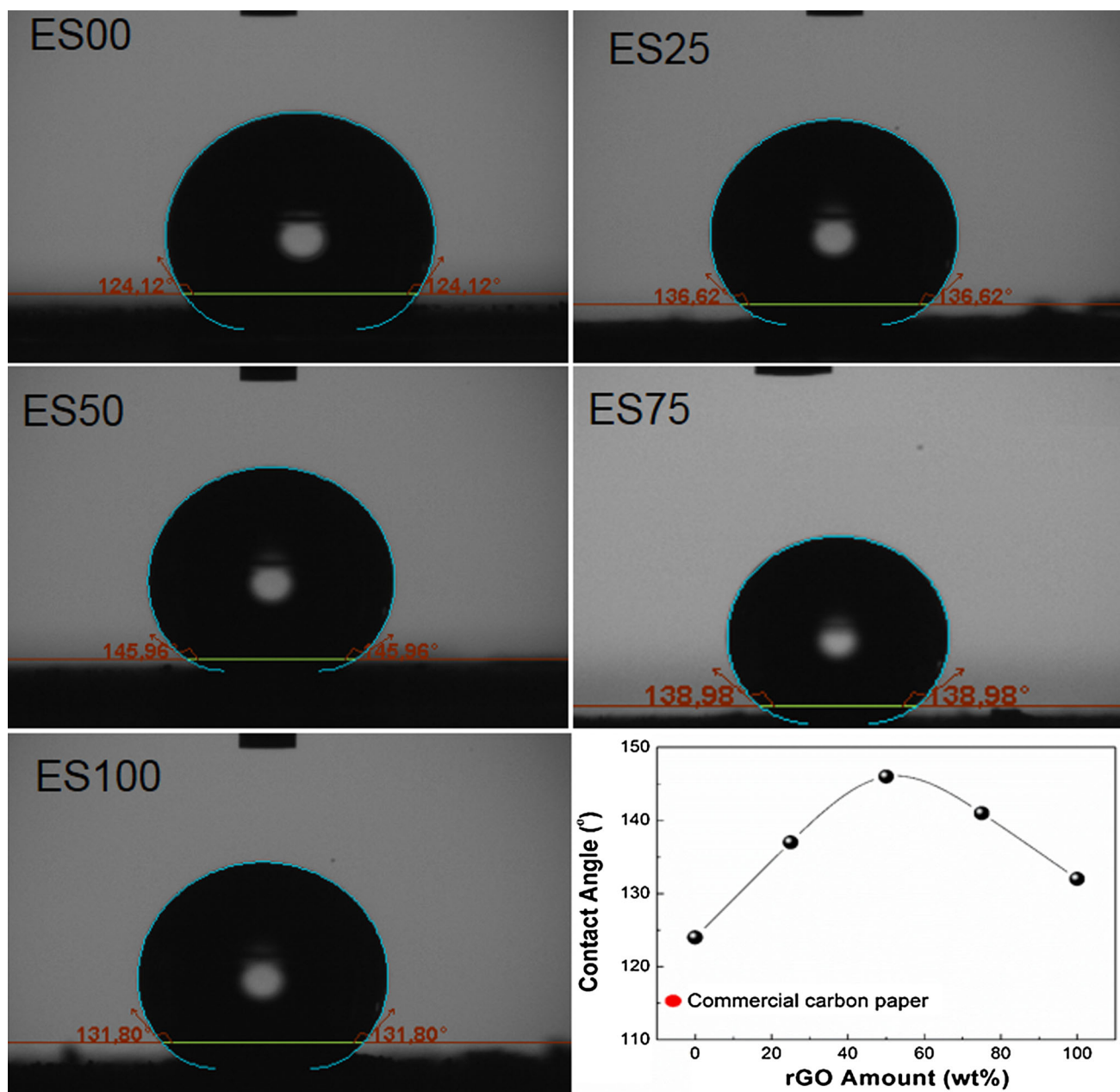


Figure 3 Contact angles of the electrospayed electrodes.

Table 2 Porosity, average, and mean pore diameter of the commercial and electrospayed electrodes

Sample	r-GO content (wt%)	Porosity (%)	Average pore diameter (μm) $d_{p, \text{ave}}$	Mean pore diameter (μm) $d_{p, \text{mean}}$
Carbon paper (MGL190)	–	77	23	29
Commercial electrode	–	67	0.5	12
ES00	0	71	13	25
ES25	25	71.5	7	25
ES50	50	71	6	25
ES75	75	71.5	11	26
ES100	100	72	13	25

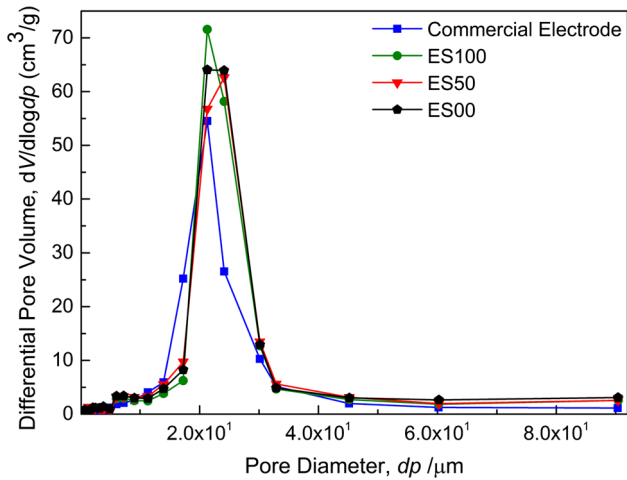
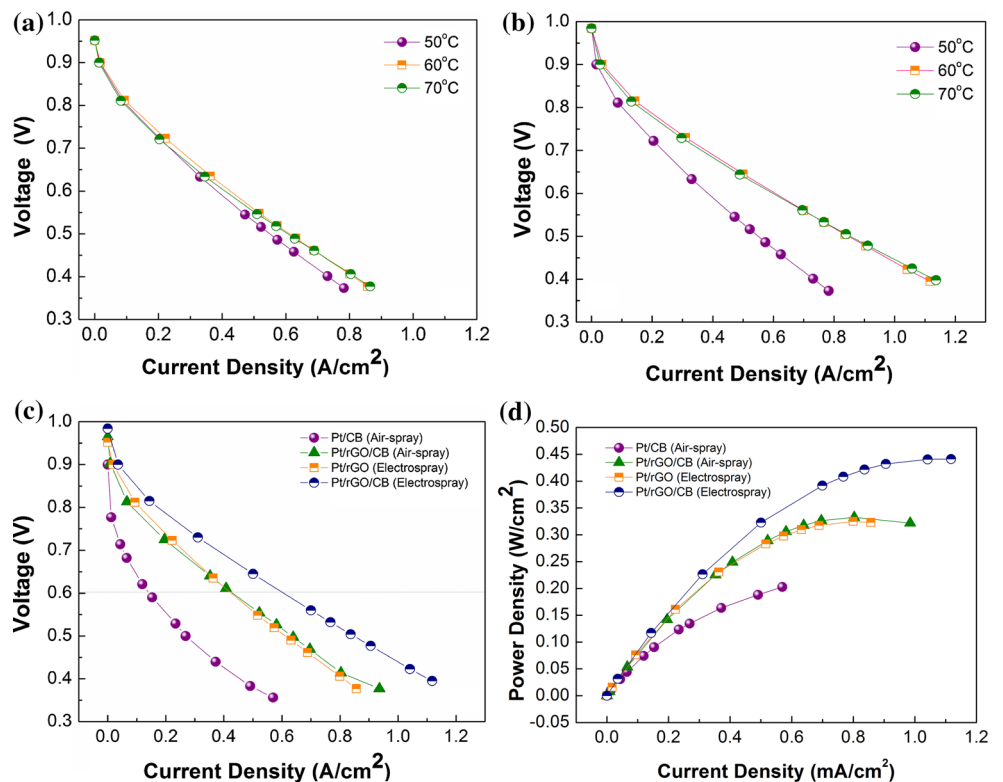


Figure 4 PSD curves ($dV/d \log dp$) for commercial electrode, ES100, ES50, and ES00.

curves for commercial electrode, ES100, ES50, and ES00. Most of the pores in commercial electrode, ES100, ES50, and ES00 are between 1.5 and 3.5, 1.9 and 3.6, 1.9 and 3.5, 1.8 and 3.6 μm , respectively. There is no significant difference in PSD values; however, it is obvious that commercial electrode pores generally located in smaller pore size region (1.8–2.6 μm) to compare the electro spray electrodes.

Figure 5 Galvanostatic polarization curves of MEAs with anode and cathode electrodes prepared via electro spraying of **a** Pt/r-GO electrocatalyst (ES00) at different temperatures, **b** Pt/r-GO/Vulcan XC-72 hybrid electrocatalyst (ES50) at different temperatures. **c** Comparison of electro sprayed and air-sprayed electrodes at 60 °C. **d** Power density curves of electro sprayed and air-sprayed electrodes.



Consequently, the smaller pore size in commercial electrode results in decrease of oxygen transport [45].

It is well known that limiting current density of the electrode layer is directly related to effective porosity controlled by water content in the gas diffusion electrodes [47, 48]. When the hydrophobicity of electrodes is examined, there is a trade-off between mass transfer benefits and ohmic losses in the catalyst layer [49]. Larger average pore diameter with evenly distributed hydrophobic content can facilitate both liquid water flow and oxygen counter flow through the electrode at a constant layer of hydrophobicity. Then, the most suitable electro sprayed electrode for fuel cell operation should be chosen by considering both hydrophobicity and average pore diameter [50]. In this regard, ES50, which has the highest static contact angle and a reasonable average pore size, was chosen for the PEM fuel cell testing.

Fuel cell performance of the electro sprayed electrodes

In this study, we aimed to maximize the electro-chemical reaction sites, and consequently to enhance fuel cell performance via hybrid support structure and electro spraying technique. The Pt loading for

Table 3 PEM fuel cell power performances of the prepared electrodes

Electrode	Max power density (mWcm ⁻²)	Max. kW/g Pt	Power density at 0.6 V (mW cm ⁻²)	kW/g Pt at 0.6 V	mA cm ⁻² at 0.6 V
Pt/CB (Air-sprayed)	203	1.0	74	0.6	190
Pt/rGO (Electrosprayed)	324	1.6	231	1.6	420
Pt/rGO/CB hybrid (Air-sprayed)	327	1.30	249	1.0	420
Pt/rGO/CB hybrid (Electrosprayed)	441	2.2	323	2.4	620

each electrode was 0.2 mg cm⁻² and the total active area was 25 cm⁻² (5 × 5 cm² each electrode) of the MEAs. As far as the fuel cell performances of MEAs based on the electrospayed anode and cathode electrodes at different temperatures are concerned, there is no prominent evaluation between cell temperatures 60 and 70 °C; thus, 60 °C was chosen as the operation temperature (Fig. 5a, b).

Figure 5c shows the comparison of fuel cell performance of electrospayed and air-sprayed electrodes at 60 °C. High fuel cell performance and power output of electrospayed electrodes based on hybrid electrocatalysts are achieved. High fuel cell performance and Pt utilization efficiency were obtained with the hybrid containing 50 wt% rGO (Table 3) at a relatively low Pt loading (0.2 mgPt cm⁻²) and operation temperature comparing with the literature [42]. The maximum power density of electrospayed Pt/rGO electrode was 324 mW cm⁻² and of Pt/rGO/CB was 441 mW cm⁻² (Fig. 5d). This achievement comes from the benefit of hybrid support morphology and electrospaying technique. The fuel cell performance improvement of the hybrid carbon support can be proved via the comparison of Pt/CB air-spray and Pt/rGO/CB electrodes performances (Fig. 5c; Table 3). Addition of graphene to the support increases the active sides while CB acts as a spacer to prevent restacking of the rGO during synthesis and ink preparation [31]. Moreover, if Pt/rGO/CB air-spray and Pt/rGO/CB electrospay MEAs are compared, the maximum Pt efficiency increases from 1.3 to 2.2 kW/gPt. The enhanced performance of the electrospayed electrodes can be attributed to facile oxygen and proton transport to the catalytic sides which is a consequence of the electrode morphology together with hybrid support structure. Thus, reactant gases can diffuse to the active catalyst sides efficiently [42, 48, 49].

Conclusions

In summary, a new fuel cell electrode structure was fabricated according to electrospaying technique using graphene and graphene hybrid for the first time in literature. After synthesis of electrocatalysts based on supported Pt nanoparticles (Pt/r-GO and Pt/r-GO/Vulcan XC-72 hybrid), these electrocatalysts, Nafion[®] ionomer and a carrier polymer PVDF-*c*-HFP were electrospayed onto the carbon paper to form the novel electrode structure. In the case of Pt/r-GO/Vulcan XC-72 hybrid electrocatalyst, r-GO and Vulcan XC-72 were mechanically mixed at different weight ratios to obtain uniform Pt distribution. As the r-GO is introduced to carbon black to form a hybrid support, micrometer-sized droplets are formed so that porosity and surface roughness increase. As a consequence, an open porous electrode structure which is favorable for mass transport is achieved by electrospaying. Contact angle measurements showed that 50 wt% r-GO-containing hybrid support exhibited the highest angle. Maximum power densities, 324 mW cm⁻² for Pt/r-GO and 441 mW cm⁻² for Pt/r-GO/Vulcan XC-72 electrospayed electrodes, were achieved at relatively low Pt loadings (0.2 mgPt cm⁻²) and temperature (60 °C). As conclusion, a superior fuel cell performance and power output of electrospayed electrodes, based on graphene and graphene hybrid compared to conventional air-sprayed electrodes, were achieved.

Acknowledgements

It is gratefully acknowledged that this research has received funding from the European Union Seventh Framework Programme under grant agreement n°604391 and n°696656 Graphene Flagship. The authors would like to thank Assoc. Prof. Dr. Muhsin

Mazman, Mutlu Akü ve Malz. San. A.Ş. R&D Center, for the assistance in porosity measurements.

References

- [1] Debe MK (2012) Electrocatalyst approaches and challenges for automotive fuel cells. *Nature* 486:43–51
- [2] Sharma R, Cherusseri J, Kar KK (2015) Polymer electrolyte membrane fuel cells: role of carbon nanotubes/graphene in cathode catalysis. *Handbook of polymer nanocomposites, processing, performance and application*. Springer, Berlin, pp 361–390
- [3] Quesnel E et al (2015) Graphene-based technologies for energy applications, challenges and perspectives. *2D Mater* 2:030204
- [4] Lee K, Zhang J, Wang H, Wilkinson DP (2006) Progress in the synthesis of carbon nanotube and nanofiber supported Pt electrocatalysts for PEM fuel cell catalysis. *J Appl Electrochem* 36:507–522
- [5] Bayrakçeken A, Smirnova A, Kitkamthorn U, Aindow M, Türker L, Eroğlu I, Erkey C (2006) Pt-based electrocatalysts for polymer electrolyte membrane fuel cells prepared by supercritical deposition technique. *J Power Sources* 179:532–540
- [6] Daş E, Gürsel SA, Şanlı LI, Yurtcan AB (2016) Comparison of two different catalyst preparation methods for graphene nanoplatelets supported platinum catalysts. *Int J Hydrog Energy* 41:9755–9761
- [7] Zeng J, Su F, Lee JY, Zhao XS, Chen J, Jiang X (2007) Method for preparing highly dispersed Pt catalysts on mesoporous carbon support. *J Mater Sci* 42(17):7191–7197. doi:10.1007/s10853-007-1571-4
- [8] Roller J, Neagu R, Orfino F, Maric R (2012) Supported and unsupported platinum catalysts prepared by a one-step dry deposition method and their oxygen reduction reactivity in acidic media. *J Mater Sci* 47:4604–4611. doi:10.1007/s10853-012-6324-3
- [9] Zhao W, Zhou X, Xue Z, Wu B, Liu X, Lu X (2013) Electrodeposition of platinum nanoparticles on polypyrrole-functionalized graphene. *J Mater Sci* 48:2566–2573. doi:10.1007/s10853-012-7047-1
- [10] Martin S, Garcia-Ybarra PL, Castillo JL (2010) Electrospray deposition of catalyst layers with ultra-low Pt loadings for PEM fuel cells cathodes. *J Power Sources* 195:2443–2449
- [11] Martin S, Martinez-Vazquez B, Garcia-Ybarra PL, Castillo JL (2013) Peak utilization of catalyst with ultra-low Pt loaded PEM fuel cell electrodes prepared by the electrospray method. *J Power Sources* 229:179–184
- [12] Wang X, Richey FW, Wujcik KH, Elabd YA (2014) Ultra-low platinum loadings in polymer electrolyte membrane fuel cell electrodes fabricated via simultaneous electrospinning/electrospraying method. *J Power Sources* 264:42–48
- [13] Tang H, Yang C, Lin Z, Yang Q, Kang F, Wong CP (2015) Electrospray-deposition of graphene electrodes: a simple technique to build high-performance supercapacitors. *Nanoscale* 7:9133–9139
- [14] Wang X, Li W, Chen Z, Waje M, Yan Y (2006) Durability investigation of carbon nanotube as catalyst support for proton exchange membrane fuel cell. *J Power Sources* 158:154–159
- [15] Rocco AM, da Silva CA, Macedo MI, Maestro LF, Herbst MH, Solórzano G, Xavier AL (2008) Purification of catalytically produced carbon nanotubes for use as support for fuel cell cathode Pt catalyst. *J Mater Sci* 43:557–567. doi:10.1007/s10853-007-1779-3
- [16] Takenaka S, Miyamoto H, Utsunomiya Y, Matsune H, Kishida M (2014) Catalytic activity of highly durable Pt/CNT catalysts covered with hydrophobic silica layers for the oxygen reduction reaction in PEFCs. *J Phys Chem C* 118(2):774–783
- [17] Li X, Wei J, Chai Y, Zhang S, Zhou M (2015) Different polyaniline/carbon nanotube composites as Pt catalyst supports for methanol electro-oxidation. *J Mater Sci* 50:1159–1168. doi:10.1007/s10853-014-8672-7
- [18] Job N, Maillard F, Marie J, Berthon-Fabry S, Pirard JP, Chatenet M (2009) Electrochemical characterization of Pt/carbon xerogel and Pt/carbon aerogel catalysts: first insights into the influence of the carbon texture on the Pt nanoparticle morphology and catalytic activity. *J Mater Sci* 44:6591–6600. doi:10.1007/s10853-009-3581-x
- [19] Zhang L, Aboagye A, Kelkar A et al (2014) A review: carbon nanofibers from electrospun polyacrylonitrile and their applications. *J Mater Sci* 49:463–480. doi:10.1007/s10853-013-7705-y
- [20] Choi HJ, Jung SM, Seo JM, Chang DW, Dai L, Baek JB (2012) Graphene for energy conversion and storage in fuel cells and supercapacitors. *Nano Energy* 1:534–551
- [21] Wang H, Maiyalagan T, Wang X (2012) Review on recent progress in nitrogen-doped graphene: synthesis, characterization, and its potential applications. *ACS Catal* 2:781–794
- [22] Antolini E, Perez J (2011) The renaissance of unsupported nanostructured catalysts for low-temperature fuel cells: from the size to the shape of metal nanostructures. *J Mater Sci* 46:4435–4457. doi:10.1007/s10853-011-5499-3
- [23] Xu C, Xu B, Gu Y, Xiong Z, Sun J, Zhao XS (2013) Graphene-based electrodes for electrochemical energy storage. *Energy Environ Sci* 6:1388–1414

- [24] Fan M, Feng ZQ, Zhu C, Chen X, Chen C, Yang J, Sun D (2016) Recent progress in 2D or 3D N-doped graphene synthesis and the characterizations, properties, and modulations of N species. *J Mater Sci* 51:10323–10349. doi:10.1007/s10853-016-0250-8
- [25] Huang X, Zeng Z, Fan Z, Liu J, Zhang H (2012) Graphene-based electrodes. *Adv Mater* 24:5979–6004
- [26] Park S, Shao Y, Wan H, Rieke PC, Viswanathan VV, Towne SA, Wang Y (2011) Design of graphene sheets-supported Pt catalyst layer in PEM fuel cells. *Electrochem Commun* 13:258–261
- [27] Li Y, Li Y, Zhu E, McLouth T, Chiu CY, Huang X, Huang Y (2012) Stabilization of high-performance oxygen reduction reaction Pt electrocatalyst supported on reduced graphene oxide/carbon black composite. *J Am Chem Soc* 134:12326–12329
- [28] Ghobadi S, Sadighikia S, Papila M, Cebeci FÇ, Gürsel SA (2015) Graphene-reinforced poly(vinyl alcohol) electrospun fibers as building blocks for high performance nanocomposites. *RSC Adv* 5:85009–85018
- [29] Ghobadi S, Mehraen S, Bakhtiari R, Shamloo B, Sadhu V, Papila M, Cebeci FÇ, Gürsel SA (2016) PVA/PANI/rGO ternary electrospun mats as metal-free anti-bacterial substrates. *RSC Adv* 6:92434–92442
- [30] Yang HN, Lee DC, Park KW, Kim WJ (2015) Platinum–boron doped graphene intercalated by carbon black for cathode catalyst in proton exchange membrane fuel cell. *Energy* 89:500–510
- [31] Şanlı LI, Bayram V, Ghobadi S, Düzen N, Gürsel SA (2016) Engineered catalyst layer design with graphene-carbon black hybrid supports for enhanced platinum utilization in PEM fuel cell. *Int J Hydrog Energy* (Published online). doi:10.1016/j.ijhydene.2016.08.210
- [32] Yu HM, Ziegler C, Oszcipok M, Zobel M, Hebling C (2006) Hydrophilicity and hydrophobicity study of catalyst layers in proton exchange membrane fuel cells. *Electrochim Acta* 51:1199–1207
- [33] Leeuwener MJ, Wilkinson DP, Gyenge EL (2015) Novel graphene foam microporous layers for PEM fuel cells: interfacial characteristics and comparative performance. *Fuel Cells*. doi:10.1002/fuce.201500031
- [34] Kozbial A, Li Z, Conaway C, McGinley R, Dhingra S, Vahdat V, Li L (2014) Study on the surface energy of graphene by contact angle measurements. *Langmuir* 30:8598–8606
- [35] Kim YG, Akbar ZA, Kim DY, Jo SM, Jang SY (2013) Aqueous dispersible graphene/Pt nanohybrids by green chemistry: application as cathodes for dye-sensitized solar cells. *ACS Appl Mater Interfaces* 5(6):2053–2061
- [36] Zhai P, Lee CC, Chang YH, Liu C, Wei TC, Feng SP (2015) A significant improvement in the electrocatalytic stability of N-doped graphene nanosheets used as a counter electrode for [Co(bpy)₃]^{3+/2+} based porphyrin-sensitized solar cells. *ACS Appl Mater Interfaces* 7(3):2116–2123
- [37] Chaparro AM, Ferreira-Aparicio P, Folgado MA, Brightman E, Hinds G (2015) Study of superhydrophobic electro-sprayed catalyst layers using a localized reference electrode technique. *J Power Sources* 325:609–619
- [38] Marcano DC, Kosynkin DV, Berlin JM, Sinitskii A, Sun Z, Slesarev A, Alemany LB, Lu W, Tour JM (2010) Improved synthesis of graphene oxide. *ACS Nano* 4:4806–4814
- [39] Şanlı LI, Bayram V, Yazar B, Ghobadi S, Gürsel SA (2016) Development of graphene supported platinum nanoparticles for polymer electrolyte membrane fuel cells: effect of support type and impregnation-reduction methods. *Int J Hydrog Energy* 41:3414–3427
- [40] Brodt M, Wycisk R, Pintauro PN (2013) Nanofiber electrodes with low platinum loading for high power hydrogen/air PEM fuel cells. *J Electrochem Soc* 160:744–749
- [41] Gatto I, Stassi A, Baglio V, Carbone A, Passalacqua E, Arico AS, Schuster M, Bauer B (2015) Optimization of perfluorosulphonic ionomer amount in gas diffusion electrodes for PEMFC operation under automotive conditions. *Electrochim Acta* 165:450–455
- [42] Brodt M, Han T, Dale N, Niangar E, Wycisk RP, Pintauro PN (2015) In-situ performance, and durability of nanofiber fuel cell electrodes. *J Electrochem Soc* 162:F84–F91
- [43] Benitez R, Soler J, Daza L (2005) Electrochemical characterisation of Pt/C suspensions for the reduction of oxygen. *J Power Sources* 151:108–113
- [44] Park S, Popov BN (2009) Effect of hydrophobicity and pore geometry in cathode GDL on PEM fuel cell performance. *Electrochim Acta* 54:3473–3479
- [45] Park S, Popov BN (2011) Effect of a GDL based on carbon paper or cloth on PEM fuel cell performance. *Fuel* 90:436–440
- [46] <http://www.avcarb.com/product/molded-graphite-laminate>. Accessed 10 Jun 2016
- [47] Springer TE, Wilson MS, Gottesfeld S (1993) Modeling and experimental diagnostics in polymer electrolyte fuel cells. *J Electrochem Soc* 140:3513–3526
- [48] Weber AZ, Darling RM, Newman J (2004) Modeling two-phase behavior in PEFCs. *J Electrochem Soc* A 151:1715–1727
- [49] Marinkas A, Hempelmann R, Heinzl A, Peinecke V, Radev I, Natter H (2015) Enhanced stability of multilayer graphene-supported catalysts for polymer electrolyte membrane fuel cell cathodes. *J Power Sources* 295:79–91

- [50] <http://www.micromeritics.com/Product-Showcase/AutoPore-IV.aspx>. Accessed 10 Jun 2016
- [51] Rosas JM, Ruiz-Rosas R, Berenguer R, Cazorla-Amorós D, Morallón E, Nishihara H, Kyotani T, Rodríguez-Mirasol J, Cordero T (2016) Easy fabrication of superporous zeolite templated carbon electrodes by electro spraying on rigid and flexible substrates. *J Mater Chem A*. 4(12):4610–4618
- [52] Tang H, Yang C, Lin Z, Yang Q, Kang F, Wong CP (2015) Electro spray-deposition of graphene electrodes: a simple technique to build high-performance supercapacitors. *Nanoscale* 7(20):9133–9139